

SECURITY CLASSIFICATION OF THIS PAGE

DTIC FILE COPY		REPORT DOCUMENTATION PAGE			
1a. REPORT SECURITY CLASSIFICATION Unclassified		1b. RESTRICTIVE MARKINGS			
2a. SECURITY CLASSIFICATION AUTHORITY		3. DISTRIBUTION / AVAILABILITY OF REPORT Approved for public release; distribution unlimited.			
AD-A197 584		5. MONITORING ORGANIZATION REPORT NUMBER(S) ARO 24076.1-EG			
6a. NAME OF PERFORMING ORGANIZATION University of Michigan		6b. OFFICE SYMBOL (if applicable)		7a. NAME OF MONITORING ORGANIZATION U. S. Army Research Office	
6c. ADDRESS (City, State, and ZIP Code) Department of Aerospace Engineering The University of Michigan Ann Arbor, MI 48109-2140		7b. ADDRESS (City, State, and ZIP Code) P. O. Box 12211 Research Triangle Park, NC 27709-2211			
8a. NAME OF FUNDING / SPONSORING ORGANIZATION U. S. Army Research Office		8b. OFFICE SYMBOL (if applicable)		9. PROCUREMENT INSTRUMENT IDENTIFICATION NUMBER DAAL03-86-K-0154	
8c. ADDRESS (City, State, and ZIP Code) P. O. Box 12211 Research Triangle Park, NC 27709-2211		10. SOURCE OF FUNDING NUMBERS			
		PROGRAM ELEMENT NO.	PROJECT NO.	TASK NO.	WORK UNIT ACCESSION NO.
11. TITLE (Include Security Classification) Analysis of Combusting High-Pressure Monopropellant Sprays					
12. PERSONAL AUTHOR(S) T.-W. Lee, J.P. Gore and G.M. Faeth					
13a. TYPE OF REPORT Reprint		13b. TIME COVERED FROM _____ TO _____		14. DATE OF REPORT (Year, Month, Day)	
15. PAGE COUNT					
16. SUPPLEMENTARY NOTATION The view, opinions and/or findings contained in this report are those of the author(s) and should not be construed as an official Department of the Army position, policy, or decision, unless so designated by other documentation.					
17. COSATI CODES			18. SUBJECT TERMS (Continue on reverse if necessary and identify by block number)		
FIELD	GROUP	SUB-GROUP			
19. ABSTRACT (Continue on reverse if necessary and identify by block number) ABSTRACT ON REPRINT					
20. DISTRIBUTION / AVAILABILITY OF ABSTRACT <input type="checkbox"/> UNCLASSIFIED/UNLIMITED <input type="checkbox"/> SAME AS RPT. <input type="checkbox"/> DTIC USERS			21. ABSTRACT SECURITY CLASSIFICATION Unclassified		
22a. NAME OF RESPONSIBLE INDIVIDUAL			22b. TELEPHONE (Include Area Code)		22c. OFFICE SYMBOL

DTIC
SELECTED
JUL 18 1988
S H

Analysis of Combusting High-Pressure Monopropellant Sprays

T. -W. LEE, J. P. GORE and G. M. FAETH *Department of Aerospace Engineering,
The University of Michigan, Ann Arbor, MI 48109-2140*

A. BIRK *U.S. Army Ballistic Research Laboratory, Aberdeen Proving Ground, MD
21005-5066*

(Received May 1, 1987; in final form August 3, 1987)

Abstract—A simplified analysis of monopropellant spray combustion was developed, based on the locally-homogeneous-flow approximation of multiphase flow theory and the thin-flame approximation of turbulent premixed flame theory. The performance of the analysis was evaluated using shadowgraphs of spray flames for a hydroxyl ammonium nitrate (HAN)-based liquid monopropellant at ambient pressures of 6–8 MPa. Predictions showed that these spray flames are very sensitive to the degree of flow development at the injector exit, with fully-developed turbulent flows requiring significantly smaller combustion volumes than slug flows having low initial turbulence levels. There was encouraging agreement between predictions and measurements; however, uncertainties concerning injector exit conditions for the experiments precluded definitive assessment of the analysis.

INTRODUCTION

Combusting monopropellant sprays have applications for throttlable thrusters, underwater propulsion systems, and regenerative liquid-propellant guns. Monopropellant spray flames are also an important fundamental problem of combustion science, as the premixed counterpart of the spray diffusion flame. Motivated by these considerations, the structure of combusting monopropellant sprays was examined during the present investigation. The main objective was to develop a simplified analysis of the process, and to evaluate predictions by comparison with measurements.

Theories of combusting monopropellant sprays are not highly developed; therefore, the present analysis was simplified. Multiphase effects were treated using the locally-homogeneous-flow (LHF) approximation of multiphase flow theory. The LHF approximation implies that relative velocities between the phases are negligible (negligible slip), yielding a single-fluid formulation which is independent of the specifics of spray breakup and initial drop-size distributions. The LHF approach generally provides useful qualitative information concerning spray structure (Faeth, 1983, 1987; Mao *et al.*, 1980, 1981; Shearer *et al.*, 1979). Additionally, Wu *et al.* (1983, 1984) report encouraging quantitative performance of LHF analysis for pressure-atomized injection at elevated pressures—conditions which are most often encountered for combusting monopropellant sprays. Finally, recent work in this laboratory (Ruff *et al.*, 1988), suggests that LHF analysis is effective for near-injector conditions in the atomization breakup regime, based on predictions and measurements of the properties of pressure-atomized water sprays in still air at normal temperature and pressure.

Address correspondence to: G. M. Faeth, 217 Aerospace Engineering Building, The University of Michigan, Ann Arbor, MI 48109-2140. Telephone: 313/764-7202.

A second major assumption of the analysis involved use of the laminar flamelet concept of premixed turbulent single-phase combustion, proposed by Bray (1978, 1980). Liquid monopropellants generally have relatively high burning rates at elevated pressure (McBratney, 1980, 1981), which implies relatively thin reaction zones; therefore, the limit of an infinitely-thin flame was used to provide a simple formulation with minimal empiricism (Bray, 1978, 1980).

The performance of the analysis was evaluated using measurements of pressure atomized sprays from a round injector passage, obtained with an apparatus developed by Birk and Reeves (1987). The measurements consisted of shadowgraphs of spray flames produced by a hydroxyl-ammonium-nitrate (HAN)-based liquid monopropellant at ambient pressures of 6-8 MPa. The data was reduced to yield mean and fluctuating liquid volume fractions as a function of position, for comparison with predictions.

Experimental and theoretical methods are described in the next two sections of the paper. Predictions of spray structure are then compared with measurements. The paper concludes with discussion of additional theoretical findings for conditions where test results are not available.

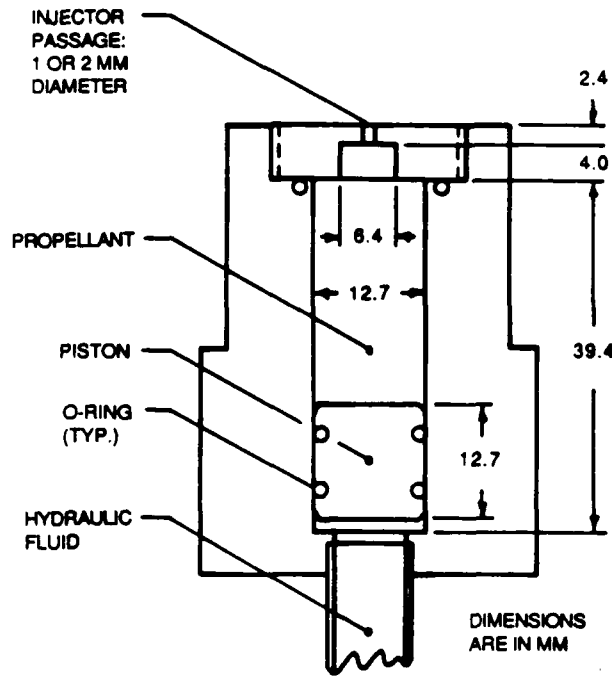


FIGURE 1 Injector assembly.

DTIC
COPY
INSPECTED

Approved for Release	<input checked="" type="checkbox"/>
by NSA on 08-01-2013	
pursuant to E.O. 13526	
DECLASSIFICATION AUTHORITY	
Derived from NSA	
Collection	
NSA	
DATE	
BY	
Dist	
A-1	20

EXPERIMENTAL METHODS

Experimental methods will be only briefly described, more details are provided by Birk and Reeves (1987). The experiments were carried out within a windowed cylindrical test chamber having an inside diameter of 57 mm and an interior length of 406 mm, yielding a volume of roughly 1050 cc. The axis of the chamber was vertical, with the pressure-atomized spray injected vertically upward along the axis. The propellant was injected into a hot precombusted gas mixture, in order to simulate injection into an adiabatic combustion environment.

The arrangement of the injector assembly is illustrated in Figure 1. The propellant was pressurized and fed through the injector passage using a hydraulically driven piston arrangement, with the hydraulic system ultimately actuated by a pneumatic system (Birk and Reeves, 1987). The injector passages were round (1 and 2 mm diameter), and were 2.4 mm long, yielding passage length-to-diameter ratios of 1.2 and 2.4. Due to steps in the propellant feed system and effects of the vena-contracta at the passage inlet, however, it is likely that the effective length-to-diameter ratios, as a measure of flow development at the passage exit, are not very well defined and are probably somewhat larger: they are taken to be in the range 2-10 in the following. The outputs of pressure transducers (Kistler 601B) were recorded to provide the test chamber pressure and the pressure differential across the injector passage.

The experiments were limited to the HAN-based monopropellant, LGP 1846, see Table I for propellant properties. The hot gas within the chamber, used to simulate an adiabatic combustion environment, was produced by spark igniting a combustible gas mixture, initially at 1 MPa, having the following composition (by volume): hydrogen, 20 percent; oxygen, 10 percent; and argon, 70 percent. Argon served as a diluent to prevent detonation of the gas mixture. Due to the relatively large surface-to-volume ratio of the test chamber, heat losses from the burning gas mixture were significant, yielding gas temperatures and pressures of roughly 1800 K and 5.5 MPa after combustion. The temperature level was roughly 10 percent below estimated adiabatic flame temperatures for the propellant (see Table I), providing a reasonable approximation adiabatic combustion conditions. The

TABLE I
Properties of LGP 1846^a

Pressure: MPa	1	10	100
<i>Reactant Properties</i>			
Density: kg m ⁻³	1430	1432	1454
<i>Product Properties</i>			
Density: kg m ⁻³	1.36	13.5	134.7
Temperature: K	2027	2039	2045
Mass Fractions: % ^b			
Water Vapor	53.8	53.9	54.0
Carbon Dioxide	24.3	24.6	24.7
Nitrogen	21.0	21.0	21.1

^aAdiabatic constant pressure combustion with the reactant at 298.15 K. Reactant composition (% by mass): hydroxyl-ammonium nitrate (HAN), 60.8; triethanol-ammonium nitrate (TEAN), 19.2; and water, 20.0.

^bMajor species only. Minor species include CO, H₂, NO, OH and O₂.

chamber pressure increased as the propellant burned: present measurements were obtained at chamber pressures of 6–8 MPa. The density of the burned gas mixture is greater than the density of the adiabatic combustion products of the propellant, due to the lower temperature and the presence of argon; therefore, the ambient density of the experiments at 6–8 MPa, approximates ambient densities for adiabatic propellant combustion at pressures of 10–13 MPa.

The combusting spray was observed using motion picture shadowgraphs. A Photec camera was used, with Kodak VNF 7240 film. Typical film speeds were 5000 frames per second. Backlighting was provided by flash sources synchronized with the camera. Maximum flash durations were less than $2 \mu\text{s}$; therefore, the image of the spray was effectively stopped on the films.

A typical spray shadowgraph is illustrated in Figure 2. The spray or liquid-containing region appears as the dark irregular zone near the center of the photograph. The boundaries of the spray are reasonably well-defined. The shadowgraphs were unusually clear in comparison to combusting hydrocarbon sprays at comparable pressures (Mao *et al.*, 1981). Factors responsible for this behavior include the absence of particulates, like soot, in the monopropellant combustion products; and the relatively uniform temperature of the combustion products, which minimizes sharp density gradients that cause irregular shadowgraph patterns. The dark zones are wispy, suggesting that the liquid behaves somewhat like tracer particles in the outer region of the liquid-containing region that can be seen on the photographs. This appearance tends to support use of the LHF approximation as a point of departure for analysis.



FIGURE 2 Photograph of combusting monopropellant spray (1 mm diameter injector, 6–8 MPa).

The motion picture films were analyzed to yield time-averaged mean and fluctuating liquid volume fractions. Maintaining the thin-flame concept, each picture frame was analyzed, assigning dark zones to unburned liquid reactant and light zones to gaseous combustion products. For each test, 15–25 frames were available for analysis during the steady flow portion of the spray combustion process. Separating dark and light zones on the film was somewhat subjective; and since the measurements correspond to line-of-sight projections, they are biased downstream and radially outward from correct point measurements of mean and

fluctuating liquid volume fractions. These effects were not quantified, but are not felt to be large in comparison to other experimental uncertainties, as will be seen subsequently.

Measurements to be considered were obtained from three tests, denoted tests 2, 4 and 7 in the following. A 1.0 mm diameter injector was used during test 2, while a 2.0 mm diameter injector was used during tests 4 and 7. In the portions of the films that were analyzed, liquid velocities were in the range 45–55 m/s for both injectors. Based on liquid properties summarized by Birk and Reeves (1987), this yields injector Reynolds numbers in the range $1-2 \times 10^4$ and Ohnesorge numbers of 0.023 (test 2) and 0.016 (tests 4 and 7). The Reynolds numbers are sufficiently high to insure reasonably turbulent flow, while the Reynolds number/Ohnesorge number combinations suggest that operation for all tests was well within the atomization breakup regime (Miesse, 1955; Ranz, 1958; Ruff *et al.*, 1988).

THEORETICAL METHODS

The analysis involves the LHF and thin-flame approximations, with turbulent mixing treated using a Favre-average turbulence model along the lines of Bray (1978, 1980) and Bilger (1976). This approach provides a useful limit and is consistent in the sense that both multiphase and chemical reaction phenomena are assumed to be controlled by turbulent mixing, vastly reducing the empiricism and amount of input data, *e.g.*, initial drop size and velocity distributions, chemical kinetic properties, etc., needed to define the problem (Bray, 1978, 1980; Faeth, 1983, 1987). As noted earlier, the LHF approach has proven to be effective for providing at least qualitative information on the structure of pressure-atomized sprays at high pressures (Faeth, 1983, 1987; Mao *et al.*, 1980, 1981; Shearer *et al.*, 1979; and Wu *et al.*, 1983, 1984); while more recent work (Ruff *et al.*, 1988) suggests that LHF analysis, similar to the approach used here, has potential for useful quantitative predictions for the near-injector region of turbulent pressure-atomized sprays in the atomization breakup regime—conditions which are met for present tests. Furthermore, the approach does not seem unreasonable in view of the wispy, gas-like, appearance of the spray-containing region seen on the spray shadowgraphs, see Figure 2.

High pressure conditions, which are generally of interest for monopropellant sprays, are favorable for application of the thin-flame approximation. Strand burning rate measurements reported by McBratney (1980, 1981) for HAN-based monopropellants suggest liquid regression rates of 20 mm/s at pressures on the order of 10 MPa. Using typical transport properties, this implies a characteristic flame thickness on the order of $1 \mu\text{m}$ (representative of both the liquid-phase preheat zone and the distance from the liquid surface to the reaction zone in the gas phase). The liquid-containing regions of the sprays had characteristic dimensions on the order of 10–100 mm, see Figure 2; therefore, the probability of a typical spatial position being within the reaction zone is quite small, justifying the thin-flame approximation. As noted earlier, the rather sharp distinction between liquid and gas, and the absence of refractive index variations in the gas-containing regions, based on photographs like Figure 2, are also supportive of this hypothesis.

It seems probable that the main structural features of turbulent pressure-atomized sprays in the atomization breakup regime are generally similar for both noncombusting and combusting monopropellant sprays. Based on what is known about noncombusting sprays, the flow should involve an all-liquid core which can

extend an appreciable distance from the injector, surrounded by a growing two-phase shear layer which originates very close to the exit of the injector (Chehroudi *et al.*, 1985; Hiroyasu *et al.*, 1982; Ruff *et al.*, 1988; Wu *et al.*, 1983, 1984). The shear layer contains irregularly-shaped liquid elements, ligaments, and drops. Upon merging the LHF and thin-flame approximations, a thin flame is assumed to cover all these surfaces: the all-liquid core, the irregularly-shaped elements, the ligaments, and the drops. Except for very near the liquid surface, the liquid is at the same state as in the injector; while beyond the outer edge of the thin flame, the gas has uniform properties equivalent to adiabatic flame conditions. Locally, the relative velocities of the phases (slip) is small.

This picture is analogous in many ways to a gaseous premixed flame in the multiple reaction sheet regime defined by Williams (1985), except that breakup of the liquid yields well-defined islands of the reactant, rather than high localized values of flame stretch in a single-phase flow. Effects of flame curvature and high flame stretch, analogous to gaseous flames, are still present in the spray, *e.g.*, reaction in the immediate vicinity of small drops and drops having very high relative velocities may be extinguished. However, due to the small flame thickness for present conditions, drops having no slip will be very small (*ca.* 1 μm in diameter) when they extinguish and will not have much effect on the mixing properties of the flow, while large slip velocities are precluded under the LHF approximation.

Other major assumptions of the analysis are as follows: (1) steady (in the mean) axisymmetric flow with no swirl; (2) low Mach number flow with negligible potential and kinetic energy changes, and negligible viscous dissipation, in the mean; (3) boundary-layer approximations apply; (4) negligible effects of radiant energy exchange; (5) equal exchange coefficients of all species and heat; and (6) high Reynolds numbers, so that laminar transport is negligible in comparison to turbulent transport. Most of these assumptions are satisfied by the conditions of present experiments. In particular, the boundary layer approximations are justified in view of the large aspect ratio of the liquid-containing region, see Figure 2. The small dimensions of the liquid-containing region and high near-injector velocities imply low radiation numbers and thus negligible effects of radiant energy exchange. The assumption of equal exchange coefficients of all species and heat is always suspect under the LHF approximation, since rates of diffusion of even small drops are small (Faeth, 1983, 1987). However, laminar exchange is not likely to be very important at Reynolds numbers on the order of 10^4 and this approximation seems no worse than other aspects of the LHF and thin-flame limits.

Under these assumptions, Bray (1978, 1980) shows that flow properties can be found by solving governing equations for conservation of mass, momentum and the reaction progress variable, in conjunction with second order turbulence model equations for turbulence kinetic energy and its rate of dissipation. The governing equations then take the following general form (Bray, 1980; Bilger, 1976; Jeng and Faeth, 1984):

$$\frac{\partial}{\partial x}(\bar{\rho}\bar{u}\phi) + \frac{1}{r} \frac{\partial}{\partial r}(r\bar{\rho}\bar{v}\phi) = \frac{1}{r} \frac{\partial}{\partial r} \left(r \frac{\mu_t}{\sigma_\phi} \frac{\partial \phi}{\partial r} \right) + S_\phi, \quad (1)$$

where $\phi = 1$ (for conservation of mass), \bar{u} , \bar{c} , k and ϵ . The source terms, S_ϕ , appearing in Eq. (1) are summarized in Table II, along with the empirical constants used during present computations. The turbulent viscosity was calculated as usual:

$$\mu_t = C_\mu \bar{\rho} k^2 / \epsilon. \quad (2)$$

The boundary conditions for Eq. (1) involve symmetry at the axis, and a constant-property ambient environment, e.g.:

$$r=0, \frac{\partial \phi}{\partial r} = 0; \quad r \rightarrow \infty, \quad \phi = 0 \text{ (for } \phi \neq \bar{c}); \quad \bar{c} = 1. \quad (3)$$

Except for C_μ , the empirical constants appearing in Table II are the same as past analysis of single- and multi-phase round jets in this laboratory (Faeth, 1983, 1987; Jeng and Faeth, 1984). These values were selected to match measurements for a variety of constant and variable density noncombusting single-phase round jets (Faeth, 1983; Jeng and Faeth, 1984). Values used, however, are not very different from those used during early work with k - ϵ turbulence models (Lockwood and Naguib, 1975).

TABLE II
Source terms in the governing equations

ϕ	S_ϕ					
\bar{c}	0					
\bar{u}	0					
\bar{c}	$C_\epsilon \bar{\rho} \bar{c} (1 - \bar{c}) \epsilon / k$					
k	$\mu_t (\partial \bar{u} / \partial r)^2 - \bar{\rho} \epsilon$					
ϵ	$(C_{1,1} \mu_t / \partial \bar{u} \partial r)^2 - C_{1,2} \bar{\rho} \epsilon \epsilon / k$					
C_μ	$C_{1,1}$	$C_{1,2}$	C_ϵ	σ_k	σ_ϵ	σ_c
0.09	1.44	1.87	1.87	1.0	1.3	0.7

Values of C_ϵ depend on the shape assumed for the reacting-mode probability density function and several turbulence modeling constants, as discussed by Bray (1980). Considering various probability density functions and estimates of empirical constants from Bray (1980), Spalding (1971), Lockwood and Naguib (1975), and Jeng and Faeth (1984), yielded values of C_ϵ of roughly two. Thus, $C_\epsilon = C_{1,2} = 1.87$ was adopted during present calculations, as a baseline. The influence of the value of C_ϵ on predictions was evaluated by parameter sensitivity calculations, to be discussed later.

It was pointed out earlier that injector exit conditions were not measured and that the flow involved complicated internal injector passages which precluded accurate estimates of exit conditions. Furthermore, computations indicated that spray properties were strongly influenced by injector exit conditions. In order to highlight this effect, a range of initial conditions was studied. This included limiting conditions of slug flow, with a uniform exit velocity and low turbulence intensities, and fully-developed pipe flow. In addition, calculations were carried out for a range of length-to-diameter ratios of the injector passage, assuming a clean entry with no vena contracta. Except for slug flow, profiles of mean velocities and turbulence quantities for these conditions were obtained from Hinze (1959) and

Schlichting (1979), given the flow rate and the diameter of the passage. The initial shear layer for the slug flow calculations was assumed to have a thickness of 0.1 percent of the passage diameter, while properties in this layer were specified similar to past work (Faeth, 1983).

Under the thin-flame approximation, the process only has two scalar states, namely, unburned reactant liquid and completely reacted gaseous products of adiabatic combustion. The properties of these states are summarized in Table I for a range of pressures. Density is the only liquid (reactant) property needed for the calculations; the values given in Table I allow for liquid compressibility and were provided by Friedman (1986). Combustion-product properties were found by assuming thermodynamic equilibrium for an adiabatic constant-pressure combustion process at the stated pressure, using the Gordon and McBride (1971) computer code.

The thin-flame approximation only admits a double-delta function probability density function for the reaction progress variable. Then, mean and fluctuating scalar properties are functions of \bar{c} , which is known from the solution of Eq. (1). The functions for various scalar properties are as follows (Bray, 1978, 1980):

$$\bar{\phi} = \phi_0(1 - \bar{c}) + \phi_\infty \bar{c}, \quad (4)$$

$$\bar{\phi} = (\phi_0 \rho_\infty (1 - \bar{c}) + \phi_\infty \rho_0 \bar{c}) / (\rho_\infty (1 - \bar{c}) + \rho_0 \bar{c}), \quad (5)$$

$$\bar{\phi}^2 = (\phi_0 - \phi_\infty)^2 \bar{c}(1 - \bar{c}), \quad (6)$$

$$\bar{\phi}^2 = \bar{\rho}^2 (\phi_0 - \phi_\infty)^2 \bar{c}(1 - \bar{c}) / (\rho_0 \rho_\infty), \quad (7)$$

where $\bar{\rho}$, needed to solve Eq. (1), can be found by setting $\phi = \rho$ in Eq. (5). Time-averaged mean and fluctuating liquid volume fractions are of particular interest, since these quantities were provided by the experiments. The equations for these properties are as follows:

$$\bar{\alpha}_l = \bar{\rho}(1 - \bar{c}) / \rho_0, \quad (8)$$

$$\overline{\alpha_l^2} = \bar{\rho}^2 \bar{c}(1 - \bar{c}) / (\rho_0 \rho_\infty). \quad (9)$$

The calculations were performed using a GENMIX algorithm due to Spalding (1978). The large density variations in the flow created problems of stability and numerical accuracy, requiring a much finer grid than is usually needed for single-phase flows. Results reported here involved 360 crosstream grid nodes; with streamwise step sizes limited to 0.3 percent of the current flow width. Doubling the number of grid nodes, in both the crosstream and streamwise directions, changed the predictions by less than 0.7 percent; therefore, the numerical accuracy far exceeds expected uncertainties of other aspects of the analysis.

RESULTS AND DISCUSSION

Evaluation of Predictions

Predictions and measurements of time-averaged liquid volume fractions along the spray axis are plotted as a function of normalized distance from the injector exit in

Figure 3. The measurements for both injector diameters are very similar when plotted in this manner. By itself, this finding suggests a mixing-controlled process for the conditions of the experiments. Similarly, predictions are also relatively insensitive to changes of injector diameters and Reynolds numbers over the range of the tests: therefore, only a single line is shown for each injector exit condition. As noted earlier, predictions were carried out for a pressure of 10 MPa, in order to match the ambient density of the experiments at 6–8 MPa. However, later results will show that the effect of pressure on the predictions for this range of conditions is small: therefore, using pressures of 6–8 MPa for the calculations would not materially influence the results.

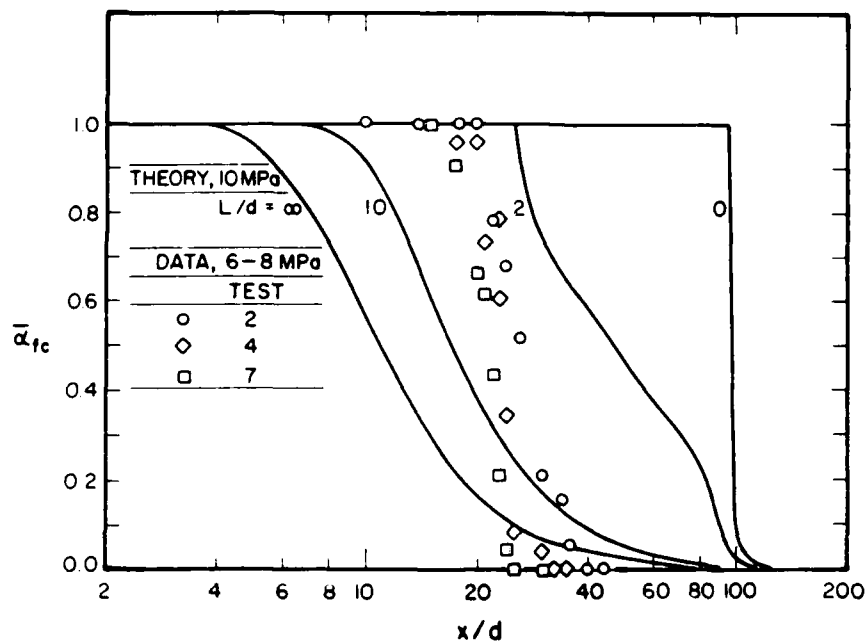


FIGURE 3 Predicted and measured variation of $\bar{\alpha}$, along axis.

In contrast to other variables, the degree of flow development at the injector exit has a strong influence on the predictions illustrated in Figure 3. For example, if the characteristic length of the combustion process is represented by the condition where $\bar{\alpha}_{fc} = 0.1$, this length is roughly five times longer for slug flow ($Ld = 0$) than for fully-developed flow ($Ld = \infty$). Due to uncertainties concerning experimental injector exit conditions, this large effect precludes definitive assessment of predictions, or any attempt to optimize C_r . Nevertheless, estimates of the properties of the test injectors suggest an effective Ld in the range 2–10; therefore, it is encouraging that predictions at these limits generally bound the measurements. The slopes of predictions and measurements are somewhat different, however, in the region where $\bar{\alpha}_{fc}$ decreases most prominently. This may be due to line-of-sight biasing and difficulties in distinguishing low concentrations of gas or liquid from

the other phase on the photographs. Effects of initial flow properties may also be a factor. Further study, and tests with better-defined injector flow conditions, required to quantify these effects.

The strong effect of initial conditions on the predicted flow properties illustrated in Figure 3 is perhaps not surprising. It is widely recognized that changes in initial conditions for single-phase turbulent jets can significantly influence the development of the flow near the injector (typically, $x/d < 20-30$). The large density of the liquid, in comparison to the gas, in a pressure-atomized spray, clearly provides the potential for carrying effects of conditions at the injector exit farther into the flow field.

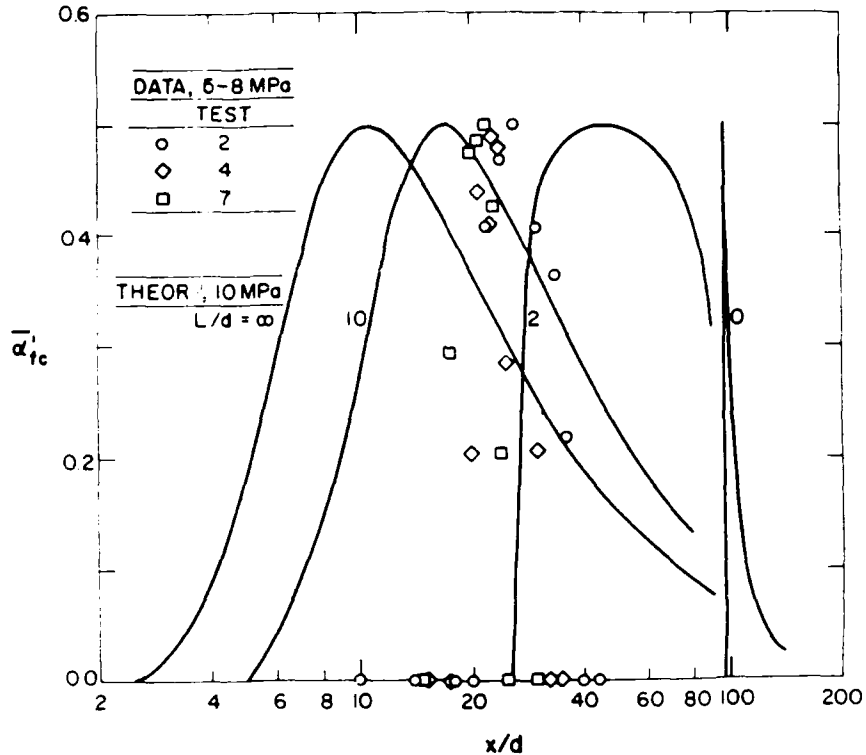
Present findings concerning the strong effect of initial flow development on the properties of combusting monopropellant sprays are also supported by recent measurements and analysis of noncombusting pressure-atomized sprays due to Ruff *et al.* (1987). Their measurements show that fully-developed flow at the injector exit causes much faster mixing than slug flow, similar to the predicted trends illustrated in Figure 3. Furthermore, LHF analysis, similar to the present approach but naturally not considering premixed combustion, provided reasonably-good estimates of the effect of flow development in the injector exit for operation in the atomization breakup regime—the regime of interest here.

Direct experimental proof of effects of initial flow development on the mixing properties of combusting monopropellant sprays is clearly needed, but the preceding discussion indicates that there is some evidence that the predicted behavior is illustrated in Figure 3 is real. This has important practical implications, since the findings suggest that fully-developed injector flows can substantially reduce combustion volumes. This can be used to provide either a more-compact combustion chamber, or to reduce tendencies for combustion instabilities by minimizing the amount of unreacted propellant within the combustion chamber at any instant.

Predicted and measured time-averaged fluctuating liquid volume fractions along the axis of the sprays are illustrated in Figure 4. Both predictions and measurements reach a maximum value of $\bar{\alpha}_l = 0.5$ at $\bar{\alpha}_l = 0.5$, which is a fundamental requirement of an intermittent (on/off) property at the thin-flame limit. Predictions and measurements were not influenced significantly by different injector sizes and Reynolds numbers, similar to findings discussed in connection with Figure 3. As before, predictions for $Ld=2$ and 10 tend to bound the measurements. However, the measured lengths of the $\bar{\alpha}_l$ profiles in the streamwise direction are narrower than predicted, possibly due to line-of-sight and photographic-contrast biasing, as discussed earlier.

Radial profiles of predicted and measured time-averaged mean and fluctuating liquid volume fractions are illustrated in Figures 5 and 6. The results are plotted as a function of rx , the similarity variable for turbulent jets, at various distance (xd) from the injector. The experimental scatter of the tests is greater for the radial profiles than the results plotted in Figures 3 and 4 for properties along the axis, particularly near the end of the liquid-containing region ($xd=20$) where the streamwise variation of flow properties is quite large, see Figure 3. Nevertheless, effects of injector diameter and Reynolds number are seen to crudely scale as a mixing-controlled process.

Predictions are illustrated in Figures 5 and 6 for the fully-developed and slug flow limits. The predictions scale in the same way as the measurements; however, the measured profiles are broader than either of the limiting predictions, even though LHF predictions generally overestimate the width of the liquid-containing

FIGURE 4 Predicted and measured variation of $\bar{\alpha}_{fc}$ along axis.

region (Faeth, 1983, 1987; Mao *et al.*, 1980, 1981; Ruff *et al.*, 1988). There are several possible explanations for this behavior. First of all, the predictions shown are not expected to properly bound measurements in the radial direction, based on the results illustrated in Figure 3. Slug flow mixes much more slowly than measured, accounting for its relatively small spread in the radial direction in comparison to measurements. Fully-developed flow mixes much more rapidly than measured, and volume fractions predicted for fully-developed flow are much lower than measured values everywhere, particularly for the results illustrated in Figure 5. Thus use of intermediate flow development conditions, *e.g.*, $Ld=2$ or 10, yields better quantitative agreement with measurements, although such matching was not pursued since injector exit conditions were uncertain in any event. Next, there was evidence of unstable flapping of the jet as a whole. Such flapping does not have a significant effect on properties in the streamwise direction, but does increase the apparent radial spread of the flow through a mechanism that is not a direct effect of turbulence. Finally, somewhat broadened measured profiles are expected, due to line-of-sight and photographic-contrast biasing, as noted earlier. In view of these considerations, the order-of-magnitude and the trends of the predictions are reasonable. However, a wider range of experimental conditions with improved control of initial conditions are needed for a more definitive evaluation of the present analysis.

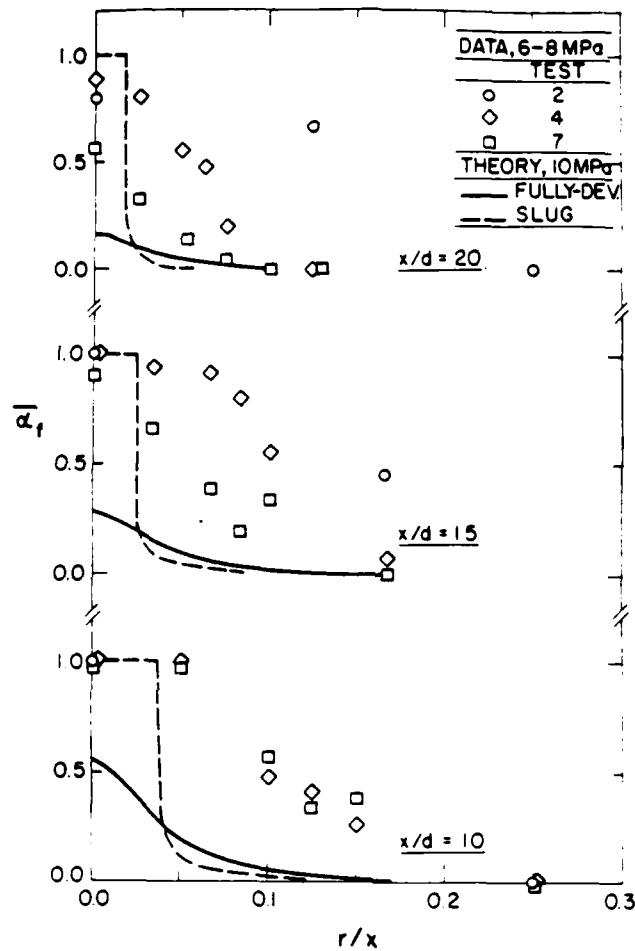


FIGURE 5 Predicted and measured radial variation of \bar{u}_z .

Additional Predictions

Since predictions were at least in qualitative agreement with the measurements, the analysis was exploited to examine some of the general properties of monopropellant sprays using the HAN-based propellant. The influence of ambient pressure and the state of flow development at the injector exit can be seen from the results illustrated in Figures 7 and 8. Predictions of $\bar{\alpha}_{ic}$ and \bar{c}_{ic} for combusting sprays are plotted at ambient pressures ranging from 10-400 MPa, which covers the range of pressures encountered for most applications of monopropellant spray flames.

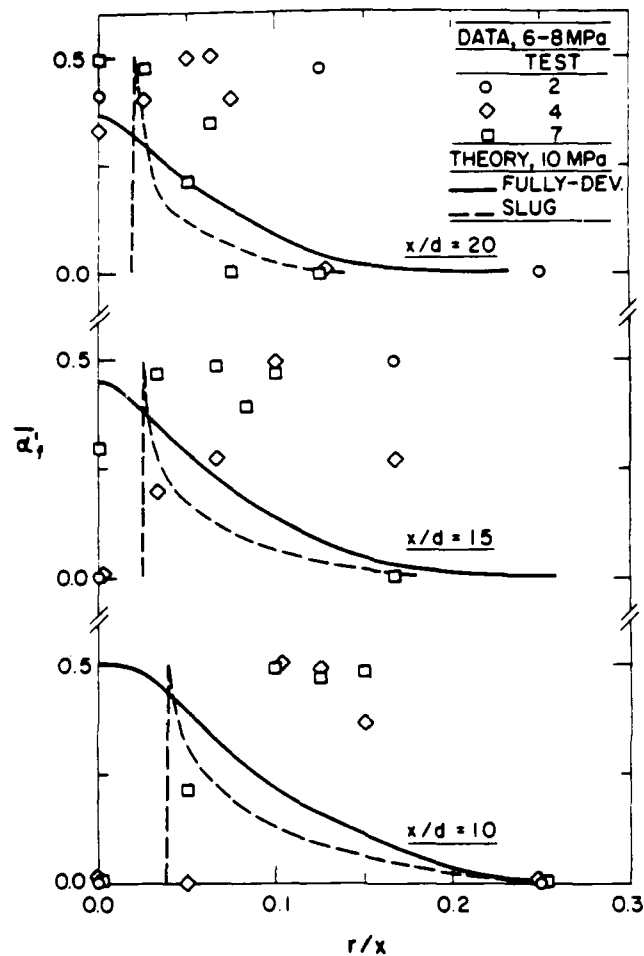


FIGURE 6 Predicted and measured radial variation of $\bar{\alpha}'$.

The findings for fully-developed injector exit conditions are illustrated in Figure 7. The Favre-averaged reaction progress variable, \bar{c}_r , is a measure of the mass of propellant reacted in the flow. Pressure clearly has a strong influence on \bar{c}_r , with the reaction nearing completion much closer to the injector at high pressures. This behaviour is caused by higher entrainment rates of the jet at higher pressures, which increases the rate of reaction at the turbulent mixing-controlled limit considered during the analysis. Existing measurements suggest that the relative entrainment rates of turbulent jets are proportional to $(\rho_v/\rho_\infty)^{1/2}$ in the similarity region of the flow see Ricou and Spalding (1961) for single-phase jets, and Faeth (1983, 1987) for multiphase jets under the LHF approximation. Jet development in the near-injector region tends to modify this behavior for the results illustrated in Figure 7; however, the trend is crudely followed, e.g., \bar{c}_r tends to approach unity at

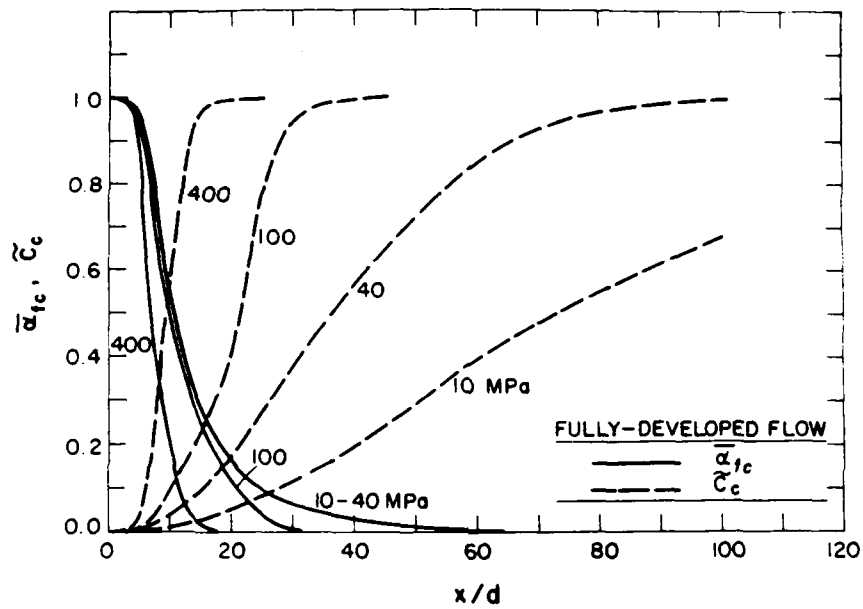


FIGURE 7 Mean scalar properties along axis at various pressures for fully-developed flow at injector exit.

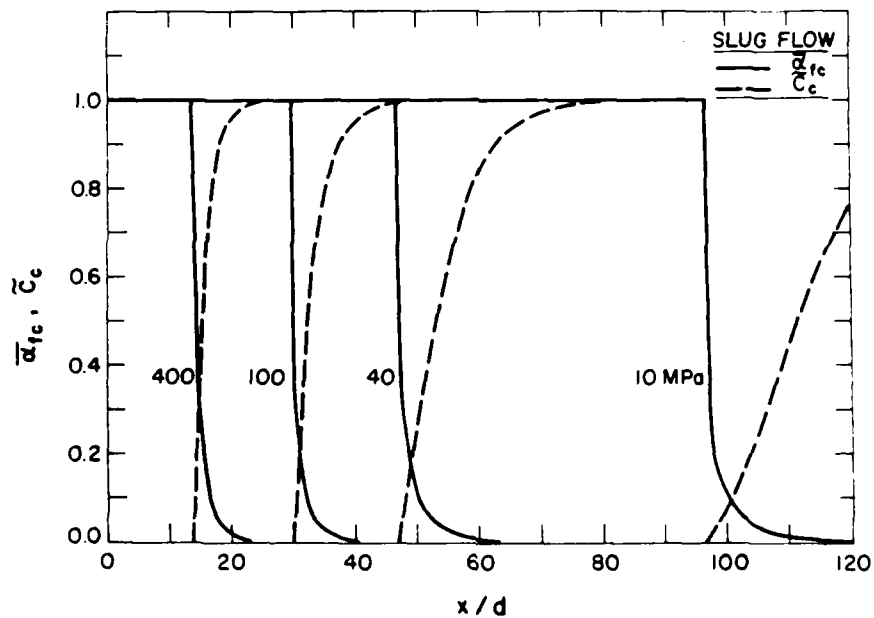


FIGURE 8 Mean scalar properties along axis at various pressures for slug flow at injector exit.

$xd = 15$ and 60 for ambient pressures of 400 and 40 MPa. In contrast, the effect of pressure on $\bar{\alpha}_r$ distributions is relatively small for pressures in the range 10 – 40 MPa. This is due to compensation of increased entrainment rates by reduced phase-density ratios as the pressure is increased.

The most obvious difference between the results for slug flow in Figure 8 and for fully-developed flow in Figure 7 is the dominating effect of an extended all-liquid potential core for slug flow. Such all-liquid cores have been observed for pressure-atomized sprays by Hiroyasu *et al.* (1982), Chehroudi *et al.* (1985) and Ruff *et al.* (1988); therefore, this behavior is not unexpected. The presence of the core tends to delay the development of the flow, particularly at low pressures. However, in spite of the core, the penetration of the sprays, represented by \bar{c}_r approaching unity, still tends to scale according to $(\rho_l/\rho_\infty)^{1/2}$, similar to the entrainment properties of fully-developed jets. In contrast, the effect of pressure on $\bar{\alpha}_r$ differs from results for fully developed flow, since the presence of the all-liquid core causes $\bar{\alpha}_r$ to vary significantly with pressure over the whole range considered in Figure 8.

Predicted isochors (for $\bar{\alpha}_r = 0.01$, which is representative of minimum liquid volume fractions generally resolvable from photographs) are illustrated in Figure 9. Results are shown for fully-developed and slug flow initial conditions at pressures in the range 10 – 400 MPa. The plots are distorted to improve their readability, e.g., the radial scale is expanded by a factor of ten in comparison to the streamwise scale. The liquid-containing region is relatively narrow in comparison to its length at all pressures, suggesting that use of the boundary-layer approximations is adequate for these flows. This is very helpful, since the turbulent premixed flame analysis has been most successful for boundary-layer flows (Bray, 1978, 1980). Increasing pressure acts to reduce the size of the region bounded by the $\bar{\alpha}_r = 0.01$ isochor; for both boundary conditions and all pressures. However, the effect of pressure on the variation of $\bar{\alpha}_r$ at higher values of this parameter, is relatively small for fully-developed flow at pressures in the range of 10 – 40 MPa, as noted earlier, see Figure 7.

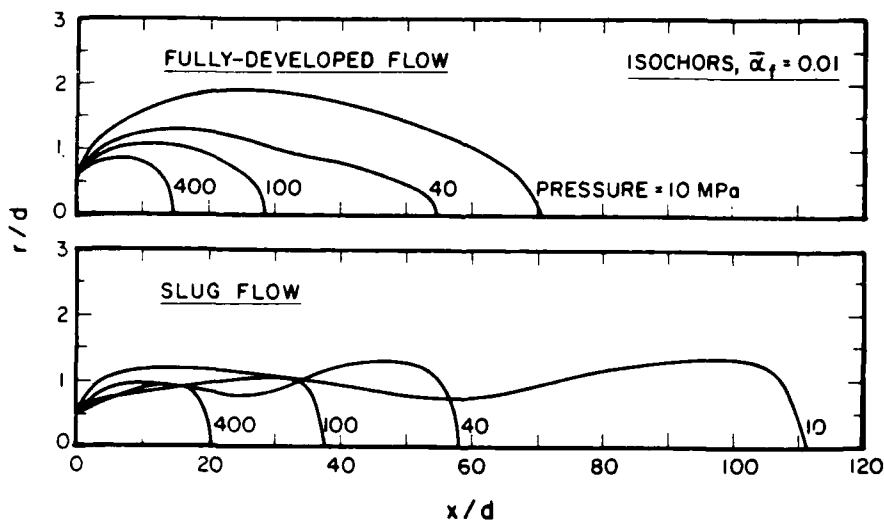


FIGURE 9 Predicted isochors ($\bar{\alpha}_r = 0.01$) at various pressures for fully-developed and slug flows at the injector exit.

Parameter Sensitivity

In addition to the extent of flow development at the injector exit, uncertainties concerning turbulence properties at the injector exit, and for other parameters of the analysis, contribute to uncertainties of predictions. This was evaluated by parametrically varying these quantities in order to observe their effect.

Table III is a summary of a portion of the parameter sensitivity results. The percent change of a given output parameter is tabulated for either a 50 percent reduction or a 100 percent increase of various input parameters, as indicated in the table. These results are for fully-developed flow at 10 MPa and $xd=20$. This position corresponds to conditions near the end of the liquid-containing region, see Figure 3. The most sensitive output parameter is \bar{a}_{lc} , with mean concentrations of unreacted liquid, $(1-\bar{c})$, and the mean velocity ratio, \bar{u}/\bar{u}_{in} , being relatively insensitive to the parameter variations. The effect of pressure is not very significant for any of the output variables at this pressure; however, this would not be the case at higher pressure levels, see Figures 7 and 8. The initial turbulence kinetic energy has the strongest influence on \bar{a}_{lc} , with a 50 percent reduction of k_0 , causing almost a 300 percent increase of \bar{a}_{lc} . This highlights the importance of turbulent mixing, which increases with increasing k_0 in the near-injector region, for the mixing-controlled turbulent reaction limit considered in the calculations. Predictably, a factor-of-two reduction of C , causes roughly a 100 percent increase in \bar{a}_{lc} , implying that this constant can be calibrated using measurements, if the fundamental approximations of the analysis, like the effect of slip, are appropriate. The other parameters considered, ϵ_0 and Re , exhibit relatively small effects on output properties for these conditions.

TABLE III
Effect of parameter variations^a

Input parameter	Output parameter (% increase)		
	\bar{a}_{lc}	$(1-\bar{c})$	\bar{u}/\bar{u}_{in}
C	110	2	-2
k_0	290	4	5
ϵ_0	-37	-3	-4
p_∞	-2	-5	-0
Re	17	1	1

^aFor fully-developed injector exit conditions at 10 MPa. Output parameter evaluated at $x/d=20$

^bParameter variations as follows: $C = C/2$, $k_0 = k_0/2$, $\epsilon_0 = \epsilon_0/2$, $p_\infty = 2p_\infty$ and $Re_0 = 2Re_0$.

CONCLUSIONS

The major conclusions of the investigation are as follows:

- 1) Use of the locally-homogenous flow and thin laminar flamelet approximations yielded encouraging agreement with measurements; however, uncertainties concerning injector exit conditions for the experiments precluded definitive assessment of the analysis.

2) Pressure-atomized monopropellant spray flames appear to be unusually sensitive to the degree of flow development and the turbulence levels at the injector exit; fully-developed flows with enhanced turbulence intensities require significantly smaller combustion volumes than slug flows with low initial turbulence intensities.

3) Predictions indicate that pressure-atomized monopropellant spray flames generally satisfy the boundary-layer approximations, except at very high pressures where phase densities become comparable. This is helpful since premixed turbulent flame analysis has been most successful for flows of this type, and the degree of empiricism needed for predictions is minimized (Bray, 1978, 1980).

4) Present predictions at the mixing-controlled limit suggest that combustion volumes decrease with increasing pressure due to increased entrainment rates; however, this effect is modified appreciably by the degree of flow development at the injector exit.

ACKNOWLEDGEMENT

This research was supported, in part, by the Army Research Office, Contract No. DAAL03-86-K-0154, under the Technical Management of D. M. Mann, and by the U.S. Army Armament of Research, Development and Engineering Center, under the Technical Management of P.-L. Lu.

REFERENCES

- Birk, A., and Reeves, P. (1987). Annular liquid propellant jets. Technical Report BRL-TR-2780, Ballistic Research Laboratory, Aberdeen Proving Ground, Maryland.
- Bilger, R. W. (1976). Turbulent jet diffusion flames. *Prog. Energy Combust. Sci.* **1**, 87.
- Bray, K. N. C. (1978). Interaction between turbulence and combustion. *Seventeenth Symposium (International) on Combustion*, The Combustion Institute, Pittsburgh, pp. 223-233.
- Bray, K. N. C. (1980). Turbulent flows with premixed reactants. In P. A. Libby and F. A. Williams (Eds.), *Turbulent Reacting Flows*, Springer, Berlin, pp. 115-183.
- Chehroudi, B., Onuma, Y., Chen, S.-H., and Bracco, F. V. (1985). On the intact core of full-cone sprays. SAE Paper 850126.
- Faeth, G. M. (1983). Evaporation and combustion in sprays. *Prog. Energy Combust. Sci.* **9**, 1.
- Faeth, G. M. (1987). Mixing, transport and combustion in sprays. *Prog. Energy Combust. Sci.*, in press.
- Friedman, E. (1986). Personal communication. Ballistic Research Laboratory, Aberdeen Proving Ground, Maryland.
- Gordon, S., and McBride, B. J. (1971). Computer program for calculations of complex chemical equilibrium compositions, rocket performance, incident and reflected shocks, and Chapman-Jouguet detonations. NASA Report SP-273, Washington.
- Hinze, J. O. (1959). *Turbulence*. McGraw-Hill, New York, pp. 491-528.
- Hiroyasu, H., Shimizu, M., and Arai, M. (1982). The breakup of high speed jet in a high pressure gaseous atmosphere. *Proceedings of the 2nd International Conference on Liquid Atomization and Spray Systems*, Madison, Wisconsin.
- Jeng, S.-M., and Faeth, G. M. (1984). Species concentrations and turbulence properties in buoyant methane diffusion flames. *J. Heat Trans.* **106**, 721.
- Lockwood, F. C., and Naguib, A. S. (1975). The prediction of the fluctuations in the properties of free, round jet, turbulent diffusion flames. *Comb. Flame.* **24**, 109.
- Mao, C.-P., Szekely, G. A., Jr., and Faeth, G. M. (1980). Evaluation of a locally homogenous model of spray combustion. *J. Energy* **4**, 78.
- Mao, C.-P., Wakamatsu, Y., and Faeth, G. M. (1981). A simplified model of high pressure spray combustion. *Eighteenth Symposium (International) on Combustion*, The Combustion Institute, Pittsburgh, pp. 337-347.
- McBratney, W. F. (1980). Windowed chamber investigation of the burning rate of liquid monopropellants for guns. Report No. ARBRL-MR-03018, Ballistic Research Laboratory, Aberdeen Proving Ground, Maryland.
- McBratney, W. F. (1981). Burning rate data, LGP 1845. Report No. ARBRL-MR-03128, Ballistic Research Laboratory, Aberdeen Proving Ground, Maryland.

- Miesse, C. C. (1955). Correlation of experimental data on the disintegration of liquid jets. *Ind. Engr. Chem.* **47**, 1690.
- Ranz, W. E. (1958). Some experiments on orifice sprays. *Can. J. Chem. Engr.* **36**, 175.
- Ricou, F. P., and Spalding, D. B. (1961). Measurements of entrainment by axisymmetric turbulent jets. *J. Fluid Mech.* **11**, 21.
- Ruff, G. A., Sagar, A. D., and Faeth, G. M. (1988). Structure and mixing properties of pressure-atomized sprays. AIAA Paper No. 88-0237.
- Schlichting, H. (1979). *Boundary-Layer Theory*, 7th ed., McGraw-Hill, New York, pp. 599-600 and 636-638.
- Shearer, A. J., Tamura, H., and Faeth, G. M. (1979). Evaluation of a locally homogeneous flow model of spray evaporation. *J. Energy*, **3**, 271.
- Spalding, D. B. (1971). Concentration fluctuations in a round turbulent free jet. *Chem. Engr. Sci.* **26**, 95.
- Spalding, D. B. (1978). GENMIX: A General Computer Program for Two-Dimensional Parabolic Phenomena. Pergamon Press, Oxford.
- Williams, F. A. (1985). *Combustion Theory*, 2nd Ed., Benjamin/Cummings, Menlo Park, CA, pp. 411-423.
- Wu, K.-J., Su, C.-C., Steinberger, R. L., Santavica, D. A., and Bracco, F. V. (1983). Measurements of the spray angle of atomizing jets. *J. Fluids Engr.* **105**, 406.
- Wu, K.-J., Coghe, A., Santavica, D. A., and Bracco, F. V. (1984). LDV Measurements of drop velocity in diesel-type sprays. *AIAA J.* **22**, 1263.

NOMENCLATURE

c	reaction progress variable
C_i	constants in turbulence model, Table II
d	injector exit diameter
k	turbulence kinetic energy
L	length of injector passage
p	pressure
r	radial distance
Re	injector exit Reynolds number
S_o	source source term, Table II
u	streamwise velocity
v	radial velocity
x	streamwise distance

Greek Letters

α	phase volume fraction
ϵ	rate of dissipation of turbulence kinetic energy
μ_t	turbulent viscosity
ρ	density
σ_t	turbulent Prandtl/Schmidt number
ϕ	generic property

Subscripts

c	centerline value
f	liquid-phase property
g	gas-phase property
$()$	injector-exit condition

Superscripts

$(-), (-')$	time-averaged mean and root-mean-squared fluctuating properties
$(\sim), (\sim')$	Favre-averaged mean and root-mean-squared fluctuating properties.